Inventory of supplemental information

Figure S1. Location of electrodes. - Linked to figure 1. This figures shows that the recordings shown in Figure 1 were obtained from the correct anatomical locations.

Figure S2. mPFC-HPC synchrony and HPC changes in theta power in the EPM and open field do not vary substantially across HPC layers. Linked to figure 3. This figure shows that the results shown in Figure 3 are independent of location within each hippocampal subregion.

Figure S3. Effects of anxiety on additional measures of synchrony. Associated with figure 3. This shows that additional measures of synchrony not shown in figure 3 are not modulated by anxiety.

Figure S4. Modulation of mPFC gamma power by hippocampal theta phase does not change in anxiety tests. Linked to figure 3. This figure shows that an additional measure of synchrony, theta-gamma modulation, does not vary with anxiety, in contrast with the results shown in Figure 3.

Figure S7. Temporal dynamics of coherence between vHPC, dHPC and mPFC. Linked to figure 1. This figure shows how coherence (shown in figure 1C) varies on a finer time scale and explains how theta-frequency coherence can be high between two pairs (mPFC-vHPC and vHPC-dHPC) but not between the third pair (dHPC-mPFC) of connected areas.

Figure S8. vHPC LFP has local relevance. Linked to figure 1. This figure shows that the local field potentials recorded in the ventral hippocampus depicted in Figure 1 affect local neuronal activity.

Figure S5. Locomotor behavior does not account for mPFC theta power increases in the open field and EPM. Linked to figure 5. This figure shows that the results shown in figure 5 cannot be accounted by overt changes in locomotor behavior.

Figure S6. Coherence with the mPFC and changes in theta power in the mHPC are intermediate between vHPC than dHPC. Associated with figure 5. This figure depicts how coherence between an intermediate hippocampal subregion and the mPFC changes with anxiety.

Figure S9. Field potential recordings and results are independent of the reference used. Associated with figure 5. This figure illustrates that the local field potential results shown in figure 5 are not specific to the choice of a particular reference electrode.

Supplementary Fig 1

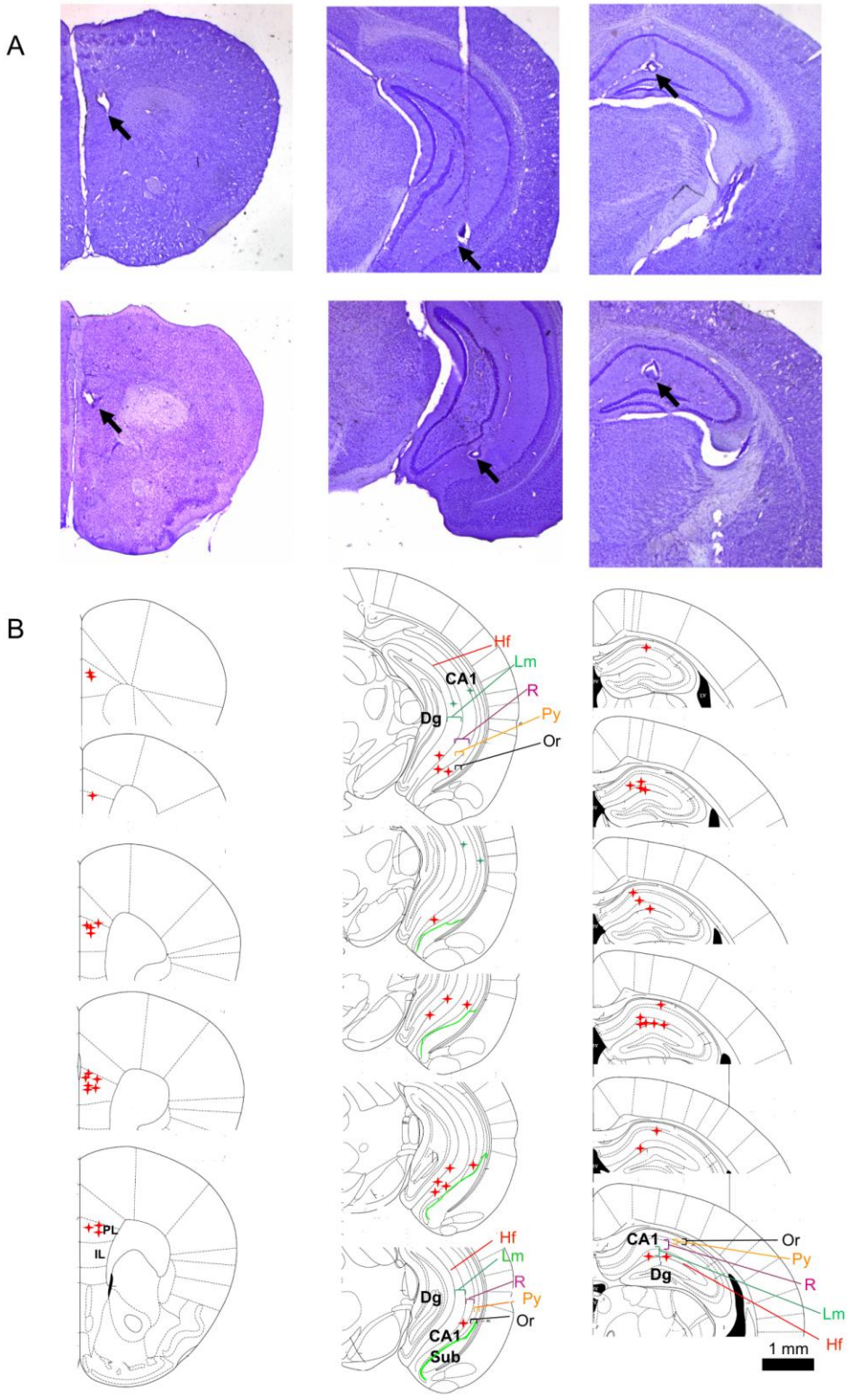

Figure S1. Location of electrodes, related to Figure 1. (A) Representative Nissl stained sections showing electrolytic lesions in mPFC (left column), vHPC (middle) and dHPC (right column). Lesion sites are indicated by arrows. (B) Diagrams show coronal sections arranged from most anterior (top) to most posterior lesions (bottom). Individual lesions are shown in red stars. Lesions of mHPC are shown as green stars. Hippocampal layers and sub-areas are shown for vHPC and dHPC sections. The border between subiculum and CA1 in vHPC sections is shown in green. Sub: subiculum, Dg: dentate gyrus, Hf: hippocampal fissure, Lm: lacunosum moleculare, R: stratum radiatum, Py: pyramidal layer, Or: stratum oriens, PL: prelimbic cortex, IL: infralimbic cortex.

Supplementary Fig 2

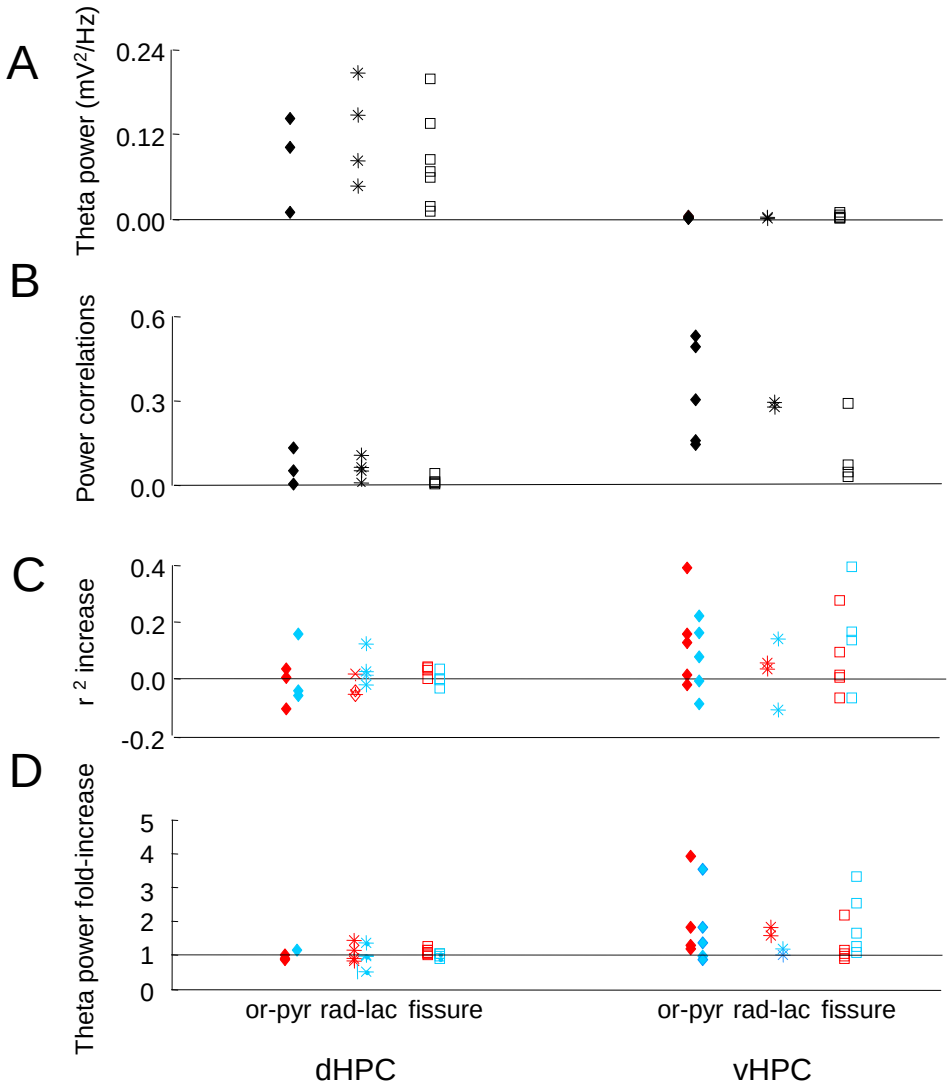

Figure S2, related to Figure 3. mPFC-HPC synchrony and HPC changes in theta power in the EPM and open field do not vary substantially across HPC layers. Plots of theta power for all layers of dHPC and vHPC. Power is higher in dHPC than vHPC in all layers (A). (B) Theta power correlations with mPFC for all layers of dHPC and vHPC are shown. (C) Change in theta power correlations with the mPFC for all layers of dHPC and vHPC. In all layers, mPFC-vHPC correlations increase in anxiogenic environments (C). (D) Theta power fold increases relative to the familiar environment in all layers of the dHPC, but not vHPC in both the open field and in the EPM are shown. Note that vHPC theta power is increased regardless of the location of the electrode. Or-pyr:oriens-pyramidal, rad-lac:stratum radiatum and lacunosum moleculare

Supplementary Fig 3

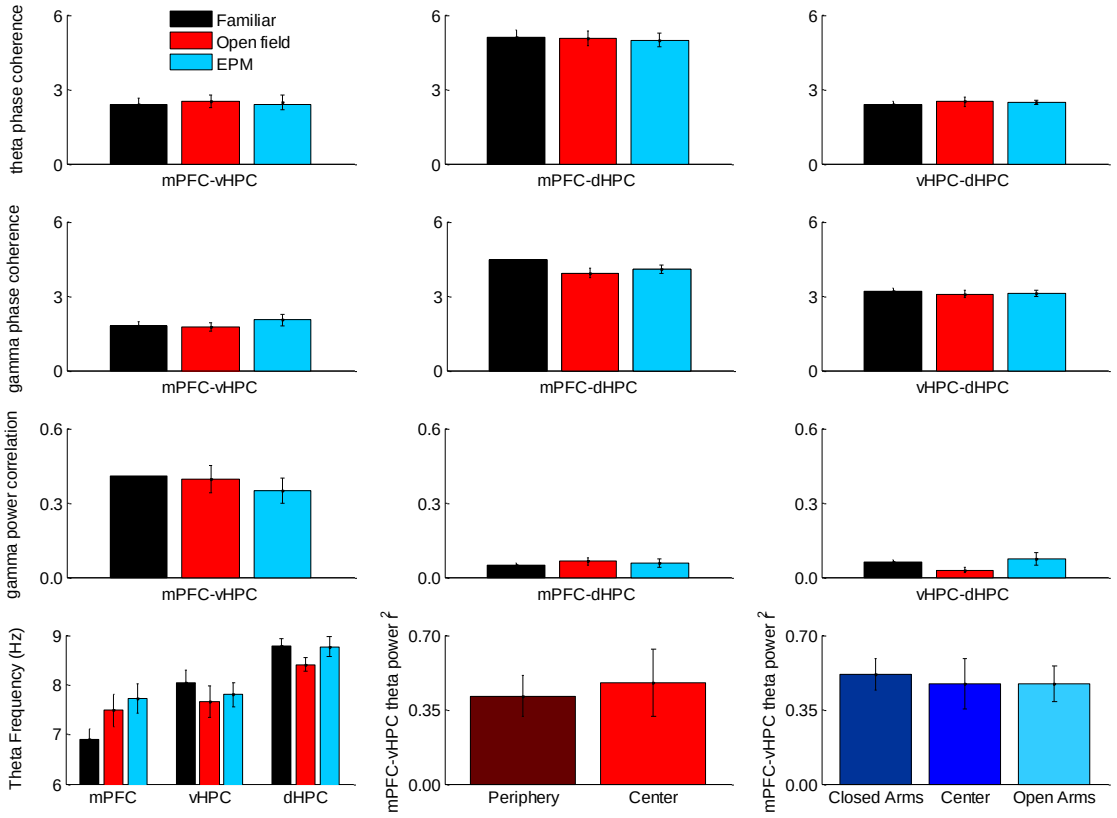

Figure S3, related to Figure 3. Effects of anxiety on additional measures of synchrony. (A) Theta phase coherence is not altered by open field or EPM across each of the brain region pairs. Phase coherence was estimated by measuring the width of the phase difference histogram at half of the peak height (see example in figure 2). Smaller widths indicate higher phase coherence. (B) Same as (A), but for gamma range. (C) Gamma range power correlations were not altered across each of the brain region pairs. Bar graphs show gamma power correlations across conditions. (D) Theta frequency across conditions for the mPFC, vHPC and dHPC. Note that theta frequency in the mPFC ini the familiar environment is significantly lower than in vHPC. With exposure to the EPM, mPFC theta increases, becoming closer to vHPC theta frequency. A similar increase with exposure to the open field did not reach statistical significance. (E-F) Theta power correlations between the mPFC and vHPC for sub-areas of the open field (E) and in the EPM (F). Error bars are ± s.e.m. *$p<0.05$ for Wilcoxon's signed rank test.

Supplementary Fig 4

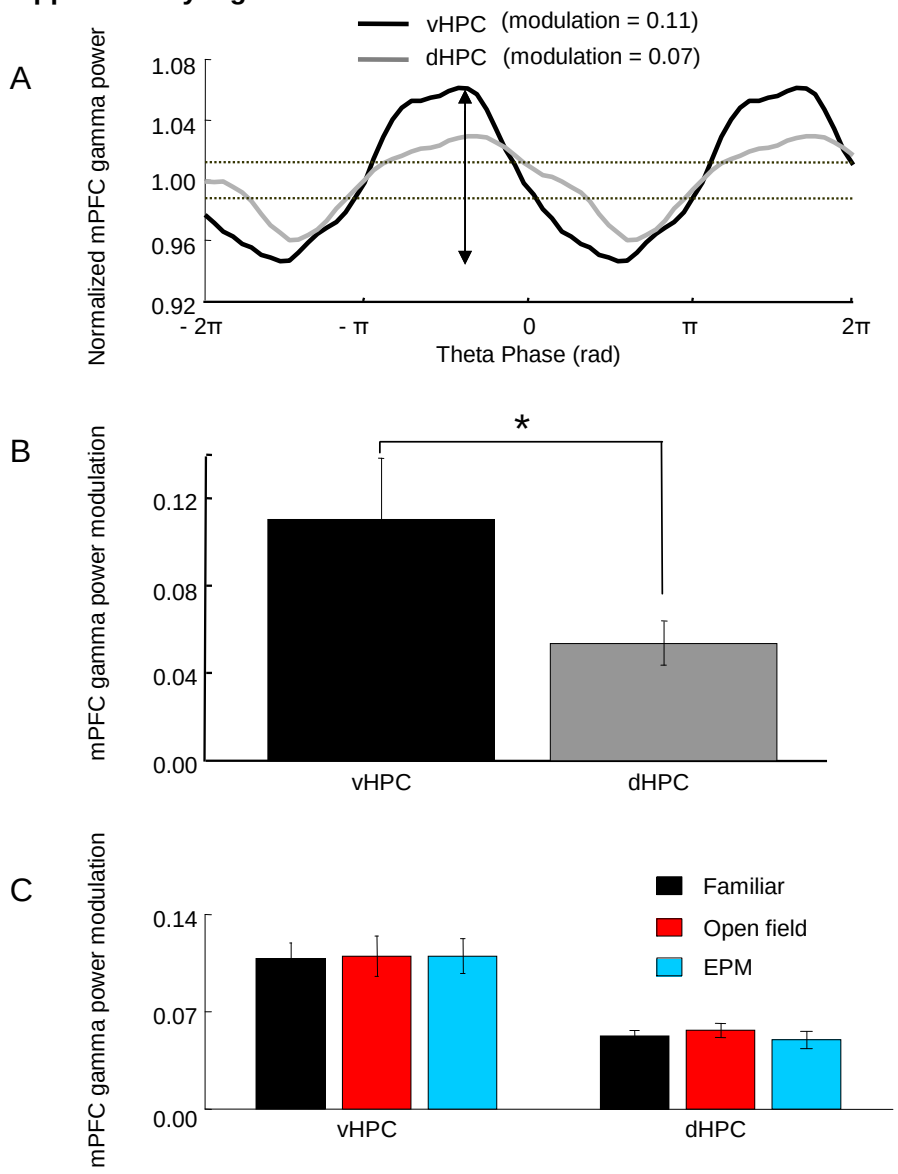

Figure S4, related to Figure 3. Modulation of mPFC gamma power by hippocampal theta phase. (A) Example traces showing modulation of normalized mPFC gamma power with vHPC (black trace) and dHPC (grey trace) theta phase. Modulation of gamma power by theta phase was calculated as being the peak to trough distance in the curve, as indicated by the double-headed arrow in the vHPC curve. Dotted lines indicate chance levels of modulation, obtained by shifting the mPFC signal by 5-10 seconds. (B) Modulation of mPFC gamma power by theta phase of vHPC (black bar) and dHPC (grey bar) averaged across 12 animals. mPFC gamma was more strongly modulated by vHPC theta than dHPC theta. (C) Data show modulation of gamma power in the mPFC by vHPC and dHPC theta phase in the familiar environment, the open field and the EPM. For simplicity, familiar environment data from the EPM and open field were averaged together. Error bars are ± s.e.m. *$p<0.05$ for a paired Wilcoxon's signed rank test.

Supplementary Fig 5

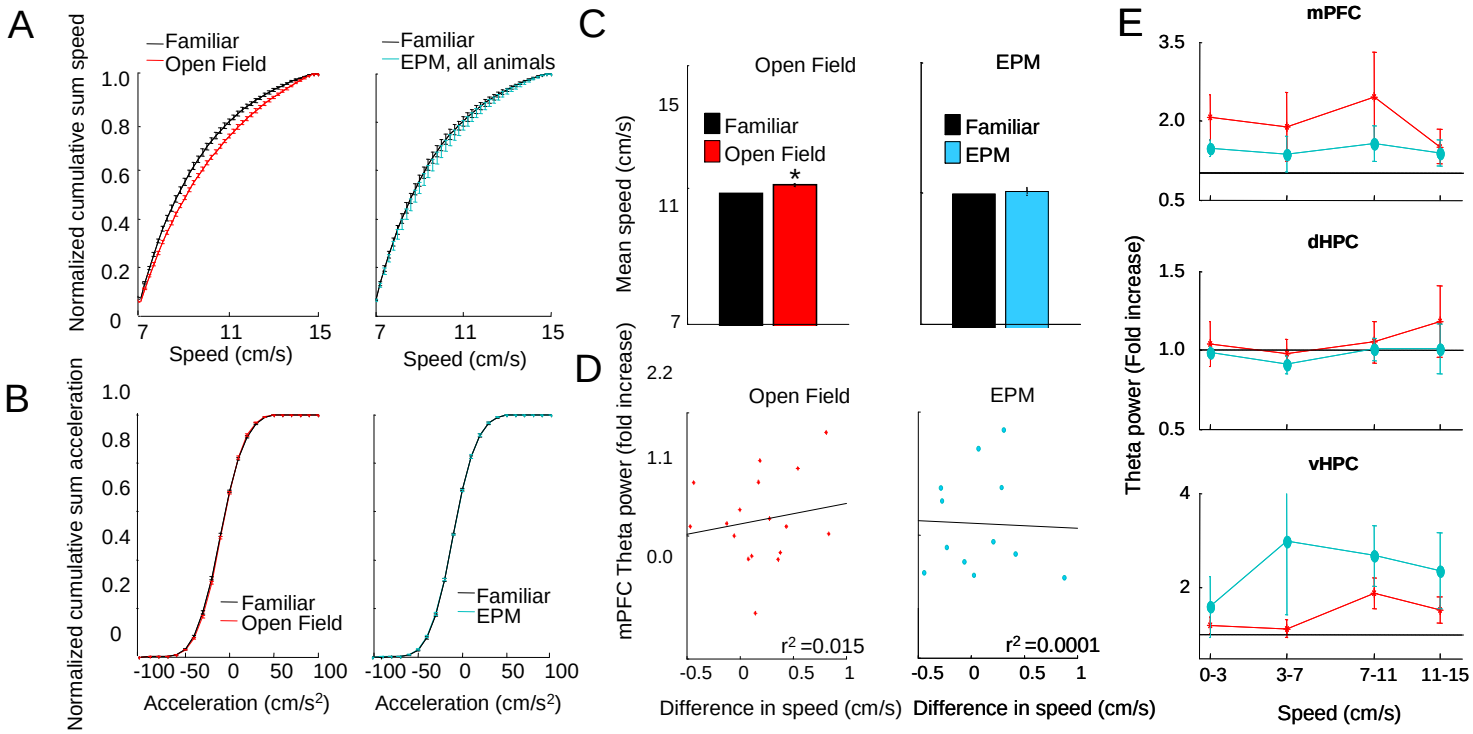

Figure S5, related to Figure 5. Locomotor behavior does not account for mPFC theta power increases in the open field and EPM. Cumulative sum distributions of speed (A) and acceleration (B) in the familiar environment (black), open field (red) and the EPM (blue) are shown. Speed distribution indicates a small increase in speed in the open field, but not in the EPM, compared to the familiar arena. (C) Relative to the familiar arena, mean speed in the 7-15 cm/s range is slightly increased in the open field, but not in the EPM. (D) Plots of mPFC theta power fold increase as a function of difference in mean speed from the familiar environment. Note that in both the open field (left panel) and the EPM (right panel) increases in mPFC theta power were not correlated with changes in mean speed relative to the familiar arena. (E) Plots showing theta power fold increase relative to the familiar environment for the open field (red) and EPM (blue), for the mPFC (top), vHPC (middle) and dHPC (bottom). Note that theta power is increased in the mPFC and vHPC in both anxiogenic environments at all speeds. $p<0.05$ for main effect of anxiety in a repeated measures ANOVA, both for mPFC and VHPC, in the open field and the EPM. There was no interaction effect between anxiety and speed. Error bars are ± s.e.m. n=18 and 12 for the open field and EPM, respectively. *$p<0.05$ in Wilcoxon's signed-rank test.

Supplementary Fig 6

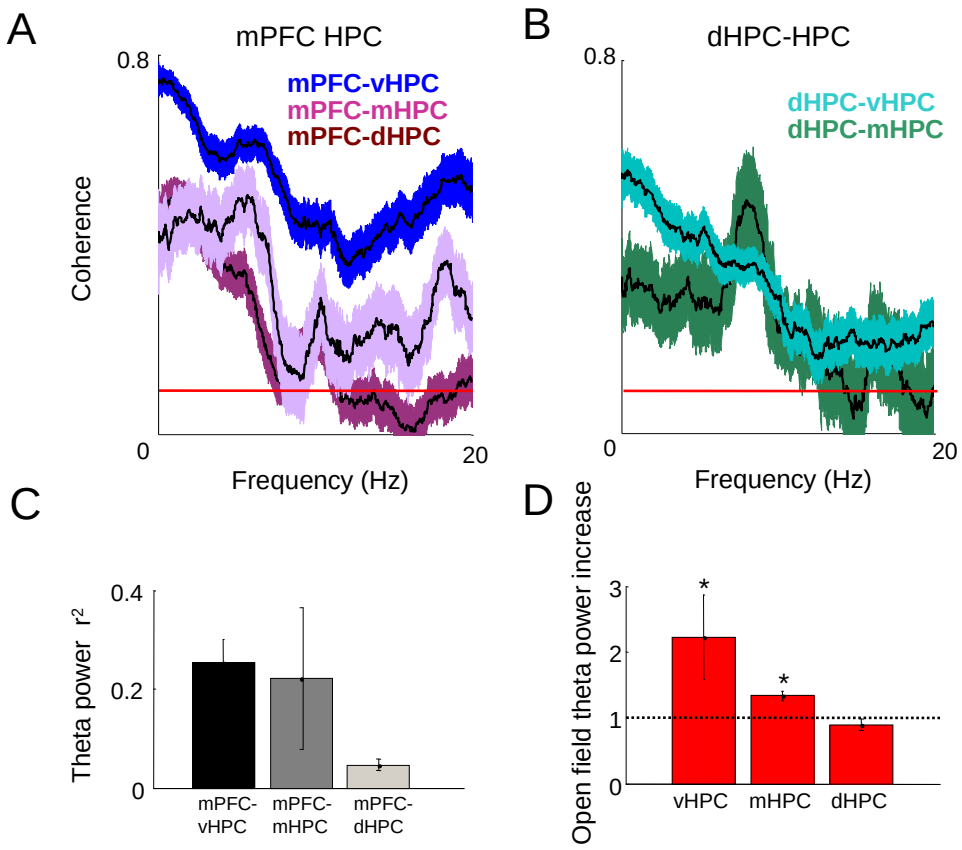

Figure S6, related to Figure 5. Coherence with the mPFC and changes in theta power in the middle hippocampus (mHPC) are intermediate between vHPC than dHPC. (A) Coherence plots of mPFC and dHPC, mHPC and vHPC. Note that coherence between mPFC and HPC increases gradually across the septo-temporal axis of the HPC, being largest with vHPC. (B) Coherence plots of dHPC with vHPC and mHPC. Theta range coherence with dHPC falls slightly across the long axis of the Hippocampus. (C) Theta power correlations of mPFC-vHPC, mPFC-mHPC and mPFC-dHPC. Correlations are high between mPFC-vHPC and mPFC-midHPC but not mPFC-dHPC. (D) Bar graphs showing fold increase of theta power in the open field relative to the familiar environment recording from the same day. Exposure to the open field increases theta power in the vHPC and mHPC relative to the familiar environment. All data shown is for the 7-15 cm/s speed range, except for theta power correlations (C), which were calculated for the length of the session. n=11, 4, 18 for the vHPC, mHPC and dHPC, respectively. Error bars are ± s.e.m. *$p<0.05$ in Wilcoxon's signed-rank test. Red lines on (A) and (B) indicate 95% significance levels.

Supplementary Fig 7

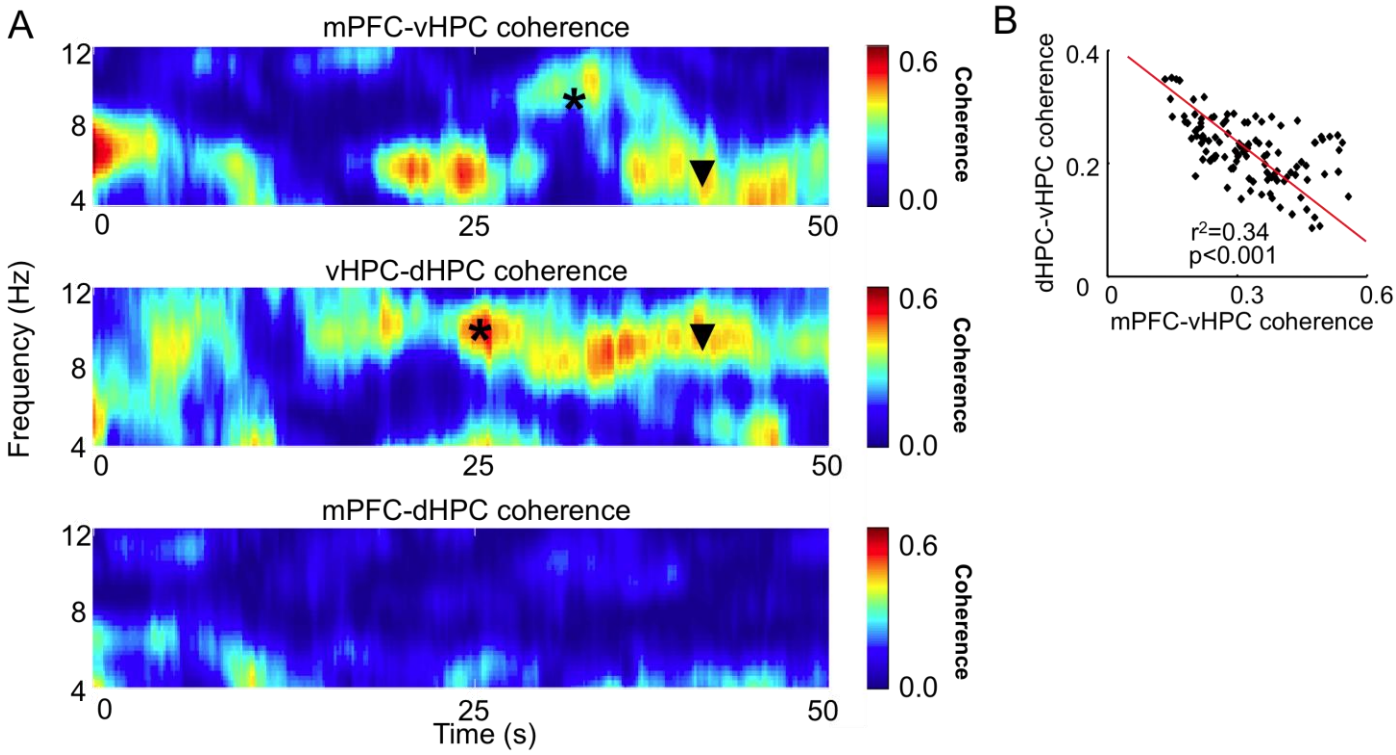

Figure S7, related to Figure 1. Temporal dynamics of coherence between vHPC, dHPC and mPFC. (A) Coherence over time plots of vHPC-mPFC (upper panel), mPFC-dHPC (middle panel) and vHPC-dHPC (lower panel) in the theta range. Higher coherence is indicated by warmer colors. Note that vHPC-dHPC and vHPC-mPFC coherence occurs either at different times (asterisks) or at different frequencies (arrowheads).Coherence was calculated on a moving 0.5 second window with 0.3 second overlap and 3700 nFFTs. Spectral densities were calculated using the multitaper method. (B) Plot showing dHPC-vHPC and mPFC-vHPC coherence across time during exploration of the familiar environment. Each point represents average coherence during 4 seconds. Note that dHPC-vHPC and mPFC-vHPC coherences are negatively correlated. Red line shows the linear fit for the scatter plot. Data was not filtered by speed and is a representative example obtained during a 10 minute familiar environment session.

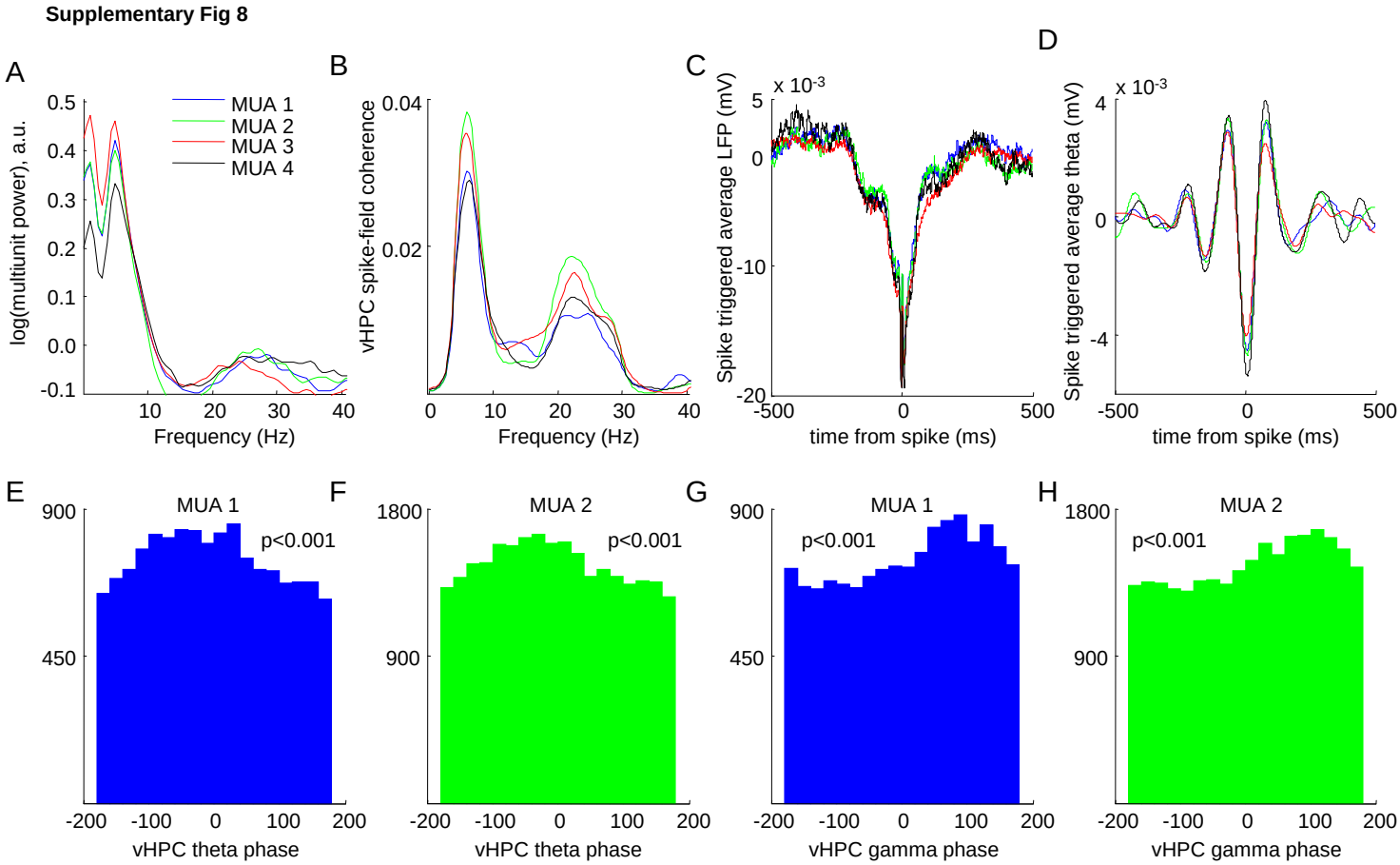

Figure S8, related to Figure 1. vHPC local field potential has local relevance. (A) Power spectra of vHPC multiunit activity (MUA). Four simultaneous recordings were made in the pyramidal layer of the vHPC, during exploration of the familiar environment. (B) Field potential–MUA coherence. Note a prominent peak at the theta range (7 Hz). (C) Spike-triggered average of the local field potential. Note that spikes tend to occur at the trough of the field. (D) Spike triggered average of theta-filtered field potential. (E) Distribution of preferred phases of vHPC MUA 1 relative to local theta oscillations. Note that spikes phase lock to the trough of vHPC pyramidal layer theta oscillations. (F) Same as (E), but for MUA 2. (G-H) Same as (E-F), but for gamma oscillations. (H) Same as (G), but for gamma oscillations. In (E-H) p values were calculated through the Rayleigh's test for circular uniformity.

Supplementary Fig 9

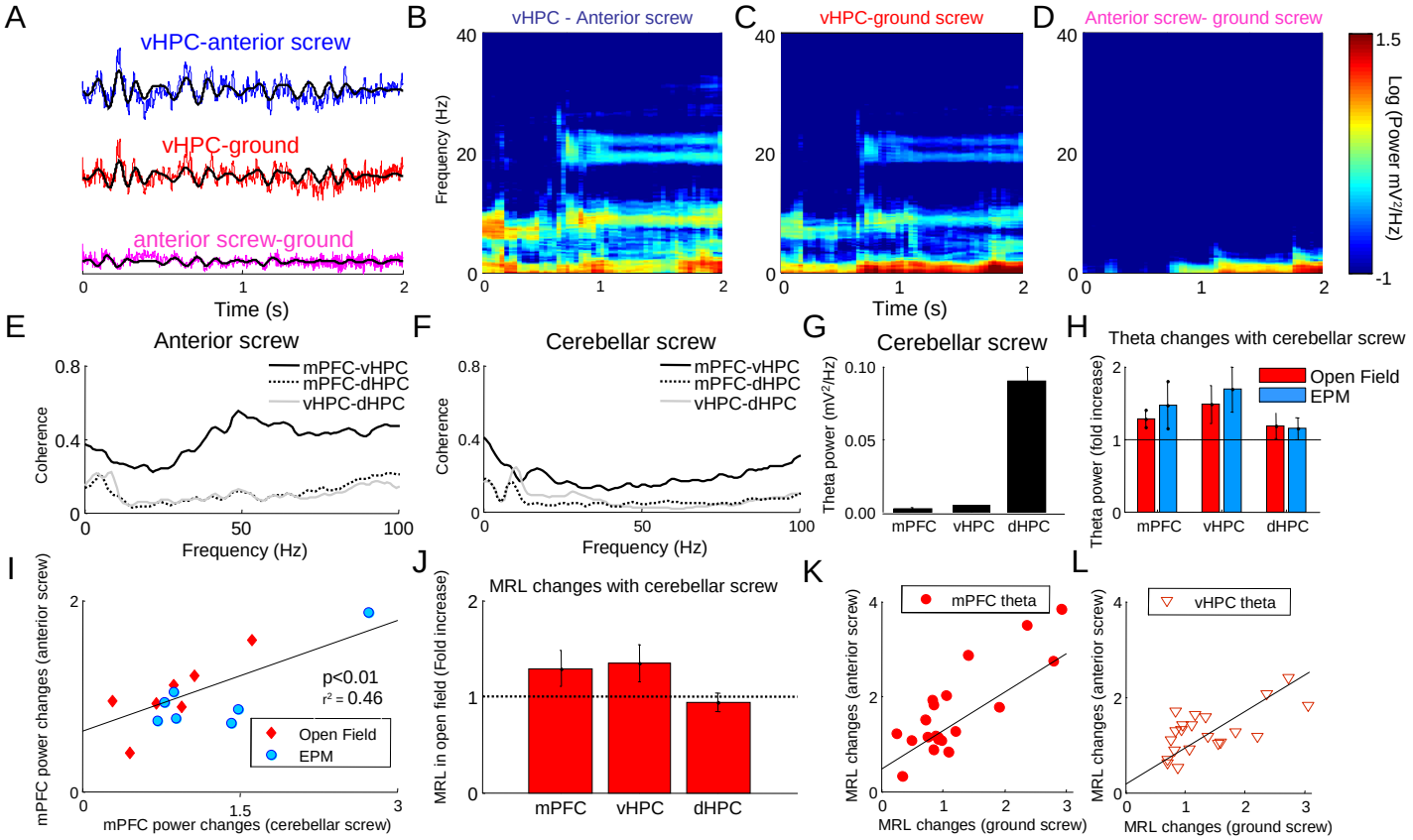

Figure S9, related to Figure 5. Main results are not reference-specific. (A) Representative traces showing the vHPC field potential recorded against the frontal (blue) or ground (red) screw. Note that both traces are very similar, indicating that the two references used are essentially identical. Accordingly, the trace of the frontal screw reference against the ground screw (pink) has overall smaller amplitude than the first two traces. (B-D) Spectrograms of the traces shown in (A). Note that the vHPC spectrogram has the same microstructure regardless of the reference used, as B and C are very similar. Furthermore, note that the anterior-screw against ground spectrogram (D) has no discernable theta-range oscillations. (E) Average coherence plots of mPFC-vHPC, mPFC-dHPC and dHPC-vHPC using an anterior screw as the reference. (F) Same as (E), but using the ground screw as a reference. Note that the mPFC is more coherent with vHPC than dHPC regardless of the reference used. (G) Theta power in the mPFC, vHPC and dHPC using the cerebellar screw as a recording reference. Note that theta power is highest in dHPC. (H) Plots of theta power increases relative to the familiar environment in the open field (red) and EPM (blue) using a cerebellar screw as a reference. Note that mPFC and vHPC theta power are increased. (I) Plot of mPFC theta power increases relative to the familiar arena with the LFP referenced either against the anterior or the cerebellar screw. Note that both measures are highly correlated in recordings performed with both references simultaneously. (J) Fold increase of MRL values in the open field relative to the familiar arena. The fold increases seen with this small sample size (n=13) agree with the full data set using the frontal reference, although they do not reach statistical significance. n=13 recordings with at least 700 spikes in each session. (K-L) Plots show fold increase of MRL relative to the familiar environment for both mPFC (K) and vHPC (L) theta oscillations. LFPs were simultaneously recorded against a cerebellar and a ground screw. Note that changes in MRL values are highly correlated across references. (E-I) Data plotted are from periods of consistent movement in the 7-15 cm/s range. (J-L) All data recorded at speeds above 4 cm/s were used. Error bars are ± s.e.m.

Short E-TOC paragraph

Synchronized activity between the ventral hippocampus and the medial prefrontal cortex during anxiety

Avishek Adhikari, Mihir A. Topiwala, Joshua A. Gordon

The ventral hippocampus is required for anxiety-like behavior. The means by which it acts are unknown. Adhikari et al. show that during anxiety, the ventral, but not dorsal hippocampus becomes more synchronized with the medial prefrontal cortex in the theta-frequency (4-12 Hz) range. Furthermore, theta power in the medial prefrontal cortex correlates with anxiety-related behaviors. These results suggest that anxiety may be mediated by theta-frequency communication between the ventral hippocampus and the medial prefrontal cortex.

(1) Neural activity in the mPFC is more synchronous with ventral than dorsal hippocampus

(2) Theta-frequency synchrony between the vHPC and mPFC increases with anxiety

(3) Theta activity in the mPFC correlates with anxiety-related behavior

(4) mPFC theta increases more strongly in a genetic model of increased anxiety